Paper

Modeling and Simulation of a Vehicle Suspension with Variable Damping versus the Excitation Frequency

Claudiu Valentin Suciu[a], Tsubasa Tobiishi[b], and Ryouta Mouri[b]

[a] *Department of Intelligent Mechanical Engineering, Fukuoka Institute of Technology, Fukuoka, Japan*
[b] *Graduate School of Engineering, Fukuoka Institute of Technology, Fukuoka, Japan*

Abstract—In this work, three types of vehicle suspensions were considered and modeled as follows: oil damper mounted in parallel with a compression helical spring, for which a Kelvin-Voigt model, consisted of a dashpot and an elastic element connected in parallel is considered; colloidal damper without attached compression helical spring, for which a Maxwell model, consisted of a dashpot and an elastic element connected in series is considered; and colloidal damper mounted in parallel with a compression helical spring, for which a standard linear model, consisted of a Maxwell unit connected in parallel with an elastic element is considered. Firstly, the vibration transmissibility from the rough road to the vehicle's body for all these suspensions was determined under the constraint that damping varies versus the excitation frequency. Then, the optimal damping and stiffness ratios were decided in order to minimize the transmissibility of vibration from the rough pavement to the vehicle's body.

Keywords—Kelvin-Voigt-Maxwell models, optimal damping and stiffness, ride comfort, transfer function of the human body.

1. Introduction

Major sources of excitation in motor vehicles are the engine, transmission system, air-conditioning system, road and aerodynamic excitations. Thus, major structural resonances and their frequency ranges are [1]: rigid body vibrations of bouncing, pitching and rolling on suspension system and wheels (0.5–2 Hz), forced vibrations of the vehicle body due to the engine shake (11–17 Hz), bending and torsional vibration of the body as a whole (25–40 Hz), as well as ring mode vibration of the passenger compartment and bending vibration of the driveline (50–100 Hz). Although resonances connected to suspension systems and wheels are in the domain of 0.5–2 Hz, structural resonances of various systems in motor vehicles are going up to 100 Hz [1]–[3]. Road excitation frequency increases with the vehicle speed and decreases with the wavelength of the road roughness; excitation frequencies 0.1–0.5 Hz are important for evaluation of the motion sickness, and the domain of 0.5–100 Hz is recommended for evaluation of the ride comfort [4], [5].

In order to improve the vehicle's ride comfort, from a technical standpoint, the suspension designer has a single alternative: to minimize the transfer function of vibration from the rough road to the vehicle's body, over the entire concerned range of frequencies (0.1–100 Hz). Usual vehicle suspensions employ hydro-pneumatic absorbers (e.g., oil [2]–[7], colloidal [8]–[14] and air dampers [2]–[7]) mounted in parallel with compression helical springs. Although the damping coefficient of the vehicle suspension is changing versus the excitation frequency [10], conventional design method is based on simplified models that assume for constant damping and elastic properties [4]. For this reason, the optimal damping and stiffness ratio, to maximize the vehicle's ride comfort, cannot be accurately predicted [15], and also discrepancies between theoretical and experimental results can be observed [16].

In this work, three types of suspensions are considered and modeled as follows: oil damper mounted in parallel with a compression helical spring, for which a Kelvin-Voigt model, consisted of a dashpot and an elastic element connected in parallel is considered; colloidal damper without attached compression helical spring, for which a Maxwell model, consisted of a dashpot and an elastic element connected in series is considered; and colloidal damper mounted in parallel with a compression helical spring, for which a standard linear model, consisted of a Maxwell unit connected in parallel with an elastic element is considered. Firstly, the vibration transmissibility from the rough road to the vehicle's body for all these suspensions is determined under the constraint that damping varies versus the excitation frequency. Then, the optimal damping and stiffness ratios are decided in order to minimize the vibration transmissibility, i.e., to maximize the vehicle's ride comfort.

2. Methods to Estimate the Ride Comfort

Perception of the vehicle's ride comfort is different from one passenger to another, depending on its taste and physical constitution. However, the ride comfort of a certain vehicle can be evaluated based on the equivalent acceleration a_c which is proportionally depending on the root-mean-square of the weighted transfer function of vibration from the rough road to the vehicle's body [4], [5]:

$$a_c \propto \sqrt{\sum_i \left[|F(f_i)||H(f_i)|\right]^2}. \quad (1)$$

Discrete frequency values are taken in the range 0.1–100 Hz, as follows: $f_i = 0.1,\ 0.125,\ 0.16,\ 0.2,\ 0.25,\ 0.315,\ 0.4,\ 0.5,\ 0.63,\ 0.8,\ 1,\ 1.25,\ 1.6,\ 2,\ 2.5,\ 3.15,\ 4,\ 5,\ 6.3,\ 8,\ 10,\ 12.5,\ 16,\ 20,\ 25,\ 31.5,\ 40,\ 50,\ 63,\ 80$ and 100 Hz. The so-called filter or weighting function $F(f_i)$ represents the vibration transfer function of the human body. For vibration transmitted in vertical direction from seat to the vehicle's rider, according to the K-factor method, the filter can be taken as [4]:

$$F(f_i) = \begin{cases} 10^{(3f_i-15)/20}, & 0 \le f_i \le 4 \\ 10^{-3/20}, & 4 \le f_i \le 8 \\ 10^{(-0.75f_i+3)/20}, & f \ge 8 \end{cases}. \quad (2)$$

On the other hand, according to ISO 2631 method, the frequency weighting can be introduced as [5]:

$$F(f_i) = \Gamma(f_i)\Delta(f_i)\frac{7.875 f_i^2}{\sqrt{0.0256 + f_i^4}}\frac{10^4}{\sqrt{10^8 + f_i^4}}, \quad (3)$$

where the functions $\Gamma(f_i)$ and $\Delta(f_i)$ can be calculated as:

$$\Gamma(f_i) = \sqrt{\frac{f_i^2 + 156.25}{0.3969 f_i^4 + 32.21875 f_i^2 + 9689.94141}}, \quad (4)$$

and:

$$\Delta(f_i) = \sqrt{\frac{0.8281 f_i^4 - 3.68581 f_i^2 + 26.1262}{0.8281 f_i^4 - 7.36421 f_i^2 + 104.29465}}. \quad (5)$$

In order to estimate the transfer function of vibration from the rough road to the vehicle's body, an adequate model should be adopted. In general, a vehicle with four wheels can be modeled as a system with 6 degrees of freedom (full-vehicle model [4], [17]). However, when the frequency in vertical direction of the vehicle's body is below 2 Hz, it is possible to neglect the rolling and to assume that the left and right parts of the vehicle are identical (half-vehicle model [17], [18]). Moreover, experience has proven that even if the pitching movement is neglected (quarter-vehicle model [17]), the ride-comfort can be predicted quite accurately. Accordingly, in this theoretical work, a quarter-vehicle moving on a rough pavement is considered as a suitable model to estimate the transmissibility and comfort.

3. Models of the Considered Vehicle Suspensions

Three types of suspensions are considered and modeled as follows: oil damper mounted in parallel with compression helical spring (Fig. 1), colloidal damper without attached compression helical spring (Fig. 2), and colloidal damper mounted in parallel with compression helical spring (Fig. 3). In (a) parts of Figs. 1–3, models with two-degrees of freedom are considered, based on the following assumptions. Travel speed is constant; there is no frontal-rear and/or axial rolling of the vehicle's body; contact between tire and road is linear; finally, suspension and tires have linear characteristics.

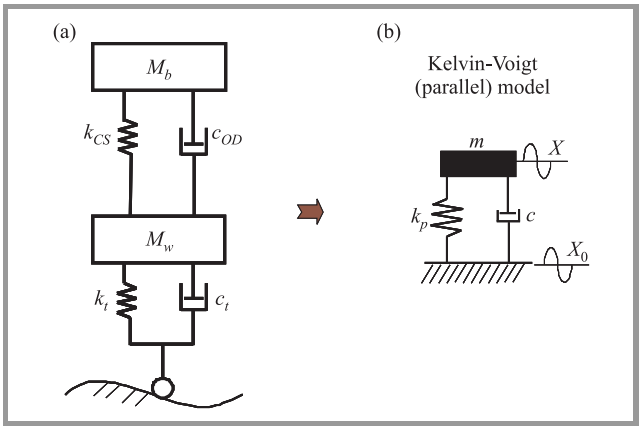

Fig. 1. Two-degrees of freedom (a) and one-degree of freedom (b) models for oil damper mounted in parallel with compression helical spring.

On the Figs. 1–3, M_b is the body (sprung) mass, M_w is the wheel (unsprung) mass, k_t is the tire spring constant, k_{CS} is the compression spring's constant, c_t is the tire damping coefficient, c_{OD} is the damping coefficient of the oil damper and c_{CD} is the damping coefficient of the colloidal damper. In the case of usual suspension (Fig. 1), compression spring provides the necessary restoring force to bring back the suspension to its initial position after a cycle of compression-extension.

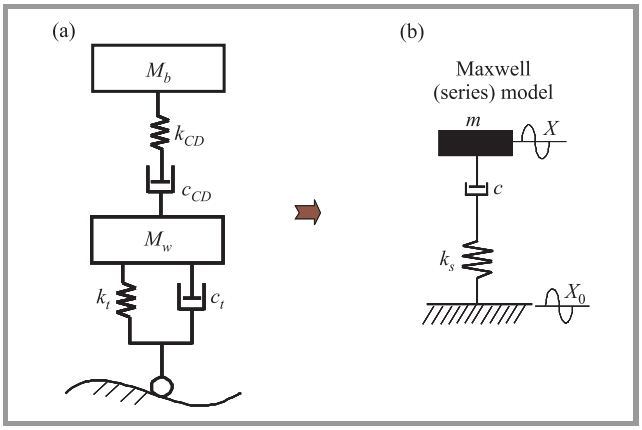

Fig. 2. Two-degrees of freedom (a) and one-degree of freedom (b) models for colloidal damper without compression helical spring mounted in parallel.

Energy of shock and vibration is mainly stored by the spring during the compression phase, and then, it is transferred to and dissipated by the oil damper during extension. On the other hand, colloidal damper is able to intrinsically provide the restoring force [15], [16] and the spring can be omitted (Fig. 2). Thus, colloidal damper is a machine element with a dual function, of absorber and spring of constant k_{CD}.

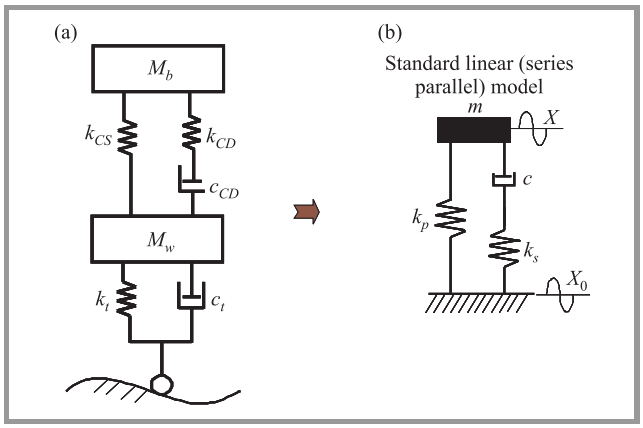

Fig. 3. Two-degrees of freedom (a) and one-degree of freedom (b) models for colloidal damper mounted in parallel with compression helical spring.

Additionally, colloidal damper is able to dissipate the energy of shock during its compression, this reducing the delay between excitation and response; since it has higher speed of reaction to excitation, one expects that the ride-comfort of the vehicle can be considerably improved.

For the model shown in Fig. 1, one observes two peaks on the graph of transmissibility of vibration from the rough road to the vehicle's body $|H|$ against the excitation frequency f, as follows: a first resonance peak at lower frequency f_n that approximately corresponds to the vehicle's body (sprung) mass, and a second resonance peak at higher frequency f_t that approximately corresponds to the wheel (unsprung) mass [19]:

$$f_n = \frac{\omega_n}{2\pi} \cong \frac{1}{2\pi}\sqrt{\frac{k_{CS}}{M_b}}, \quad f_t = \frac{\omega_t}{2\pi} \cong \frac{1}{2\pi}\sqrt{\frac{k_t}{M_w}}. \tag{6}$$

Generally, one observes two opposite requirements in the design of actual vehicle suspension (oil damper mounted in parallel with spring): large damping c_{OD} is desirable at lower frequency f_n to reduce the first resonant peak, but on the other hand, low damping c_{OD} is needed at higher frequency f_t to reduce the second resonant peak [19]. One observes from Eq. (1) that, in order to improve the vehicle's ride comfort, from a technical standpoint, the suspension designer has a single alternative: to minimize the transfer function of vibration from the rough road to the vehicle's body, over the entire concerned range of frequencies (0.1–100 Hz). One way to reduce damping in a passive manner at higher frequencies is to use a "relaxation damper", where the dashpot c_{OD} is replaced by a Maxwell unit, consisted of a dashpot, e.g., c_{CD} and a spring, e.g., k_{CD} mounted in series (Figs. 2 and 3). Since the peak at lower frequency f_n is critical, the model with two-degrees of freedom can be further simplified to a quarter-vehicle with one-degree of freedom ((b) parts of Figs. 1–3), by defining the equivalent mass m of the vehicle, the equivalent spring constant of the parallel k_p and serial k_s elastic elements, and the equivalent damping coefficient c of the dashpots as follows:

$$\begin{cases} m = M_b + M_w \\ \dfrac{1}{k_p} = \dfrac{1}{k_t} + \dfrac{1}{k_{CS}}\dfrac{M_b}{M_w} \\ k_s = k_{CD} \\ c = c_{OD} + c_t \quad \text{or} \quad c = c_{CD} + c_t \end{cases}. \tag{7}$$

Thus, the considered suspensions can be modeled as follows:

- Oil damper placed in parallel with a compression spring can be described by a Kelvin-Voigt model, consisted of a dashpot and an elastic element connected in parallel (Fig. 1).
- Colloidal damper without attached compression spring can be described by a Maxwell model, consisted of a dashpot and an elastic element connected in series (Fig. 2).
- Colloidal damper mounted in parallel with a compression helical spring, can be described by a standard linear model, consisted of a Maxwell unit connected in parallel with an elastic element (Fig. 3).

4. Modeling of the Variable Damping

Variation of the damping ratio ξ versus the excitation frequency can be taken as:

$$\xi = \xi_n \left(\frac{\omega}{\omega_n}\right)^i, \tag{8}$$

where the natural circular frequency ω_n and the damping ratio at resonance ξ_n can be calculated as:

$$\omega_n = \sqrt{\frac{k}{m}}, \quad \xi_n = \frac{c}{2\sqrt{km}}. \tag{9}$$

Subscripts p or s will be added to ω_n and ξ_n in the sections below, according to the type of spring coefficient used for their calculus: k_p (parallel) or k_s (serial), respectively. The exponent i can be taken:

- as $i = 1$ for oil dampers at higher piston speeds [4];
- as $i = 0$ for oil dampers at lower piston speeds (see the simplified model of constant damping [2]–[4]);
- as $i = -1$ for colloidal dampers [15], [16], as well as control active oil dampers at higher piston speeds [17], [18].

5. Transmissibility of Vibration from the Rough Pavement to the Vehicle Body

Transfer function of vibration $|H|$ from the rough road to the vehicle's body is defined as the ratio of the amplitude X

of the equivalent mass m to the amplitude X_0 of the displacement excitation produced by the rough pavement (see Figs. 1–3):

$$|H| = X/X_0. \tag{10}$$

5.1. Kelvin-Voigt (parallel) Model

In the case of Kelvin-Voigt model (Fig. 1), consisted of a dashpot and an elastic element connected in parallel, the transfer function of vibration is calculated by using Eq. (11). Then, variation of vibration transmissibility versus frequency $\omega/\omega_{n,p} = f/f_{n,p}$ is shown in Fig. 4 for $i=0$ and various damping ratios, and in Fig. 5 for different exponents i.

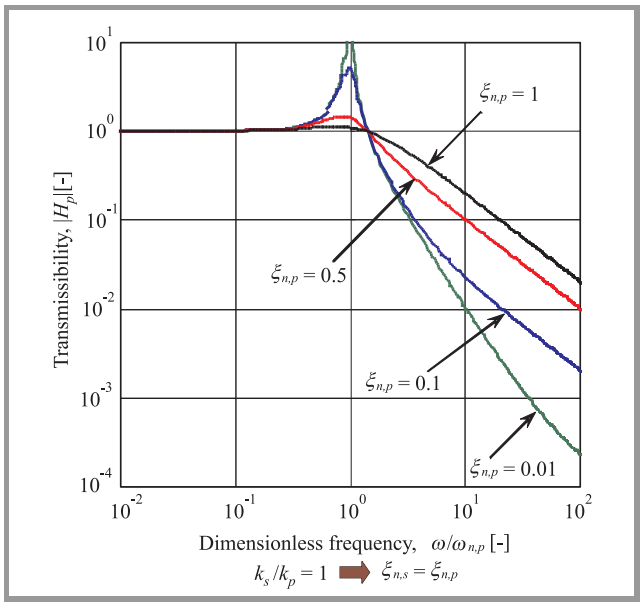

Fig. 4. Variation of transmissibility versus dimensionless frequency in the case of Kelvin-Voigt model for $i = 0$ and various damping ratios.

$$|H_p| = \sqrt{\frac{1+\left[2\xi_{n,p}\left(\frac{\omega}{\omega_{n,p}}\right)^{i+1}\right]^2}{\left[1-\left(\frac{\omega}{\omega_{n,p}}\right)^2\right]^2+\left[2\xi_{n,p}\left(\frac{\omega}{\omega_{n,p}}\right)^{i+1}\right]^2}} \tag{11}$$

From Eq. (11) and Fig. 5 one observes that for a given $\xi_{n,p}$ the resonant peak has the same height regardless the type of absorber:

$$|H_p| = \left(\frac{\omega}{\omega_{n,p}} = 1\right) = \sqrt{1+\frac{1}{4\xi_{n,p}^2}}, \quad (\forall) i. \tag{12}$$

Additionally, from Eq. (1) and Fig. 4 one observes that:

$$|H_p| = \left(\frac{\omega}{\omega_{n,p}} = \sqrt{2}\right) = 1, \quad (\forall)\xi_{n,p}, \quad (\forall) i. \tag{13}$$

Since all curves $|H_p|$ are above 1 for $\omega < \sqrt{2}\omega_{n,p}$ and below 1 for $\omega > \sqrt{2}\omega_{n,p}$one concludes that the critical frequency $\sqrt{2}\omega_{n,p}$ separates regions of amplification and attenuation, regardless the type of absorber and its damping ratio. When $\xi_{n,p} = 0$ the highest decay rate of transmissibility is obtained in the frequency domain $\omega > \sqrt{2}\omega_{n,p}$ but this is accompanied by very large amplitudes near the resonance. Consequently, one observes that there are two opposite requirements in the design of classical parallel-type suspension: large damping is desirable at lower frequencies to reduce the resonant peak, but on the other hand, low damping is needed at higher frequencies to minimize the transmissibility. Traditional way to reduce damping at higher frequencies in a passive manner [19] is to replace the dashpot by a Maxwell unit consisted of a dashpot and a spring connected in series (Fig. 3). Since the resonant peak is the same for all values of the exponent i but the decay rate in the higher frequency domain is the highest for $i = -1$ (Fig. 5), one arrives to a different way of reducing damping at higher frequencies in a passive manner. Concretely, the traditional oil damper ($i = 0$) can be replaced by a colloidal damper ($i = -1$), which has a dynamic behavior resembling the well-known case of structural damping.

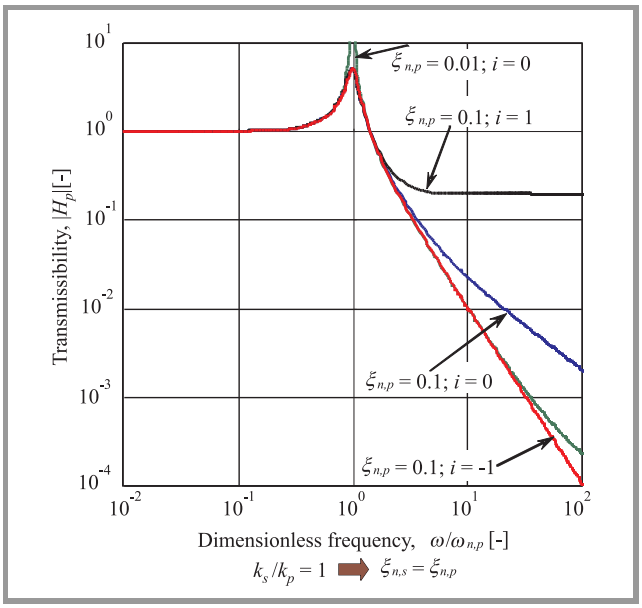

Fig. 5. Variation of transmissibility versus dimensionless frequency in the case of Kelvin-Voigt model for various exponents i.

5.2. Maxwell (series) Model

In the case of Maxwell model (Fig. 2), consisted of a dashpot and an elastic element connected in series, the transfer function of vibration can be calculated as:

$$|H_s| = \frac{2\xi_{n,s}\left(\frac{\omega}{\omega_{n,s}}\right)^i}{\sqrt{\left(\frac{\omega}{\omega_{n,s}}\right)^2+\left[2\xi_{n,s}\left(\frac{\omega}{\omega_{n,s}}\right)^i\right]^2\left[1-\left(\frac{\omega}{\omega_{n,s}}\right)^2\right]^2}}. \tag{14}$$

Then, variation of vibration transmissibility versus frequency $\omega/\omega_{n,s} = f/f_{n,s}$ is shown in Fig. 6 for $i = 0$ and various damping ratios, and in Fig. 7 for different values

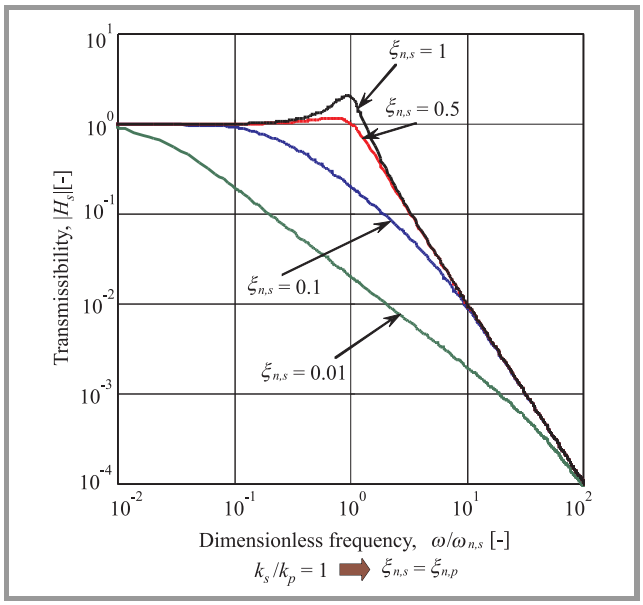

Fig. 6. Variation of transmissibility versus dimensionless frequency in the case of Maxwell model for $i = 0$ and various damping ratios.

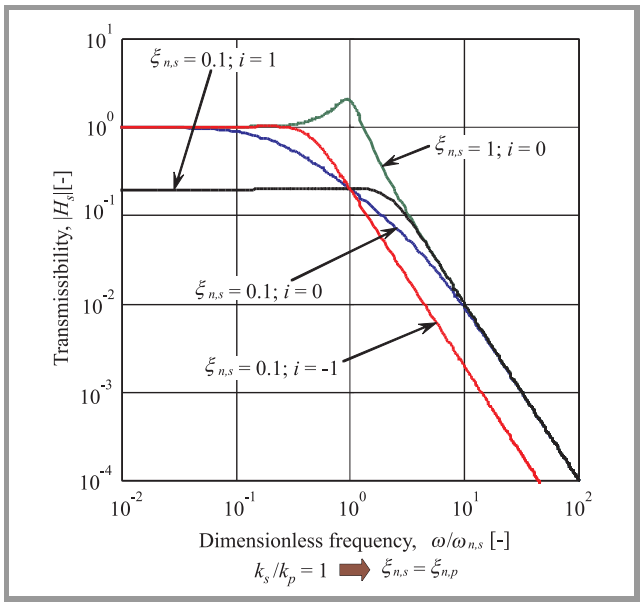

Fig. 7. Variation of transmissibility versus dimensionless frequency in the case of Maxwell model for various exponents i.

of the exponent i. Note that transmissibility reduces as the damping ratio $\xi_{n,s}$ decreases (Fig. 6); the lowest transfer of vibration is achieved in the region $\omega < \omega_{n,s}$ for the highest exponent i, but in the region $\omega > \omega_{n,s}$ for the lowest exponent i (Fig. 7).

From Eq. (14) one observes that for a given damping the "resonant peak" has the same height regardless the absorber:

$$|H_s|\left(\frac{\omega}{\omega_{n,s}} = 1\right) = 2\xi_{n,s}, \quad (\forall) i. \tag{15}$$

5.3. Standard Linear (series-parallel) Model

In the case of standard linear model (Fig. 3), consisted of a Maxwell unit connected in parallel with an elastic element, the transmissibility can be calculated as:

$$|H_{sp}| = \sqrt{\frac{\left(\frac{k_s}{k_p}\right)^2 + \left[2\xi_{n,p}\left(\frac{\omega}{\omega_{n,p}}\right)^{i+1}\left(1+\frac{k_s}{k_p}\right)\right]^2}{\left\{\frac{k_s}{k_p}\left[1-\left(\frac{\omega}{\omega_{n,p}}\right)^2\right]\right\}^2 + \left\{2\xi_{n,p}\left(\frac{\omega}{\omega_{n,p}}\right)^{i+1}\left[1+\frac{k_s}{k_p}-\left(\frac{\omega}{\omega_{n,p}}\right)^2\right]\right\}^2}}. \tag{16}$$

Then, variation of vibration transmissibility versus frequency $\omega/\omega_{n,p}$ is shown in Fig. 8 for a stiffness ratio $k_s/k_p = 1$, an exponent $i = 0$, and different damping coefficients $\xi_{n,p}$.

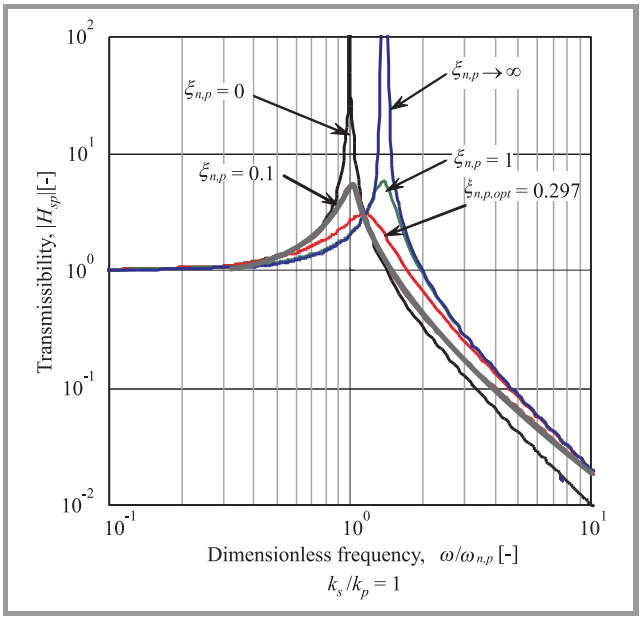

Fig. 8. Variation of transmissibility versus dimensionless frequency in the case of standard linear (serial-parallel model) for $i = 0$ and various damping ratios.

Figure 8 shows that for $\xi_{n,p} = 0$ (undamped suspension) a resonant peak occurs at $\omega = \omega_{n,p}$ and for $\xi_{n,p} \to \infty$ (over-damped suspension) a different resonant peak occurs at higher frequency ($\omega = \omega_{n,p}\sqrt{1 + k_s/k_p}$). The lowest curve, that displays the lowest resonant peak at the junction point of the graphs shown for undamped and over-damped suspensions, corresponds to the optimal damping ratio $\xi_{n,p,opt} = 0.297$ which minimizes the vibration transmissibility.

6. Optimal Design of Serial-Parallel Suspension

Analyzing the structure of Eq. (16), one concludes that the resonant peaks shown by Fig. 8, i.e., the undamped peak occurring at $\omega = \omega_{n,p}$ and the over-damped peak occurring at $\omega = \omega_{n,p}\sqrt{1 + k_s/k_p}$ are not depending on the type

of damper (value of the exponent i). Based on the theory of the maximum achievable modal damping [19], in the same way as found in Fig. 8, for any given stiffness ratio k_s/k_p one always finds an optimal damping ratio $\xi_{n,p,opt}$ that minimizes the vibration transmissibility, as follows:

$$\xi_{n,p,opt} = \frac{1}{2}\frac{k_s}{k_p}\left(1+\frac{k_s}{k_p}\right)^{-3/4}, \quad (\forall) i. \tag{17}$$

Figure 9 illustrates a monotonous variation of the optimal damping ratio $\xi_{n,p,opt}$ versus the stiffness ratio k_s/k_p.

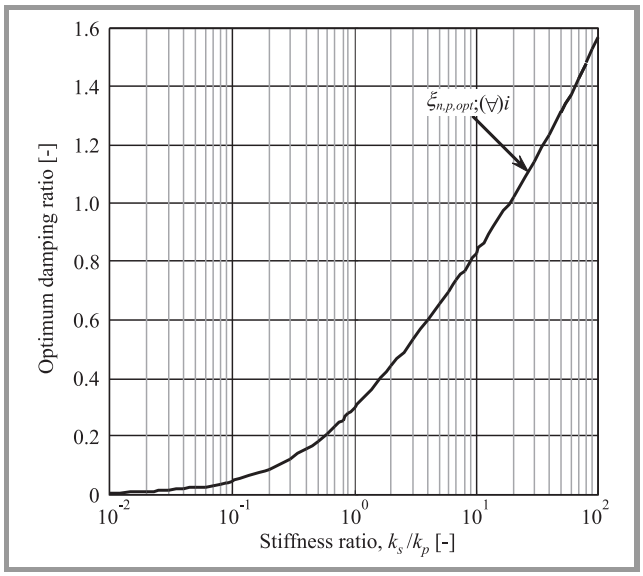

Fig. 9. Variation of the optimal damping ratio versus the stiffness ratio to minimize the transmissibility, for all types of dampers ($i = -1, 0, 1$).

Next, in order to obtain the optimal stiffness ratio, i.e., the optimal ratio of the colloidal spring's constant to the compression spring's constant, one compares the vibration transmissibility obtained with the parallel, series, and series-parallel models for values of the stiffness ratio ranging from low to high (e.g., $k_s/k_p = 0.01 - 100$). It can be shown that at augmentation of the stiffness ratio the resonant peak decreases, but the transmissibility in the higher frequency domain increases. In order to maximize the vehicle's ride-comfort in the whole frequency domain, one integrates the graphs showing the variation of vibration transmissibility versus frequency. In this way, as Fig. 10 illustrates, one obtains the variation of area below the graph of transmissibility versus the stiffness ratio, both for the case without filter and for the cases when filters (see Eq. (2) for the K-factor method, and Eq. (3) for the ISO 2631 method) are used to account for the effects of vibration on the human body. All the graphs shown in Fig. 10 are convex (valley-like) curves. Stiffness ratio corresponding to the deepest point of the valley represents the optimal stiffness ratio that minimizes the vibration transmissibility, i.e., maximizes the ride-comfort over the whole frequency range. Thus, based on the positions of minima observed in Fig. 10, the optimal stiffness ratio $(k_s/k_p)_{opt}$ is decided

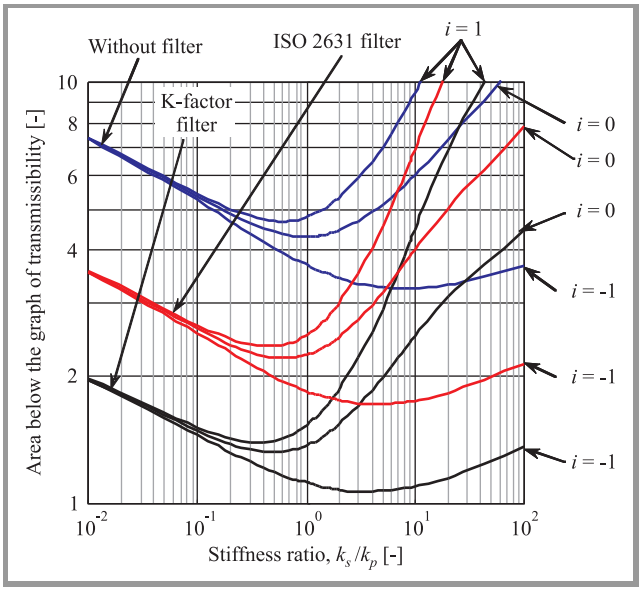

Fig. 10. Decision of the optimal stiffness ratio to achieve minimal transmissibility, i.e., maximal ride comfort for various dampers and filters.

for various types of absorbers ($i = -1, 0, 1$), both for the case without filter and for the cases when filters are used to account for the effects of vibration on the human body (see Table 1).

Table 1
Optimal stiffness ratio for various types of dampers and different methods to estimate the ride comfort

Optimal $(k_s/k_p)_{opt}$	Type of damper		
	$i = -1$	$i = 0$	$i = 1$
Without filter	8.0	1.0	0.6
ISO 2631 filter	5.0	0.6	0.5
K-factor filter	4.0	0.5	0.4

7. Conclusion

In this work, three types of suspensions were considered and modeled as follows: oil damper mounted in parallel with a compression helical spring, for which a Kelvin-Voigt model, consisted of a dashpot and an elastic element connected in parallel was considered; colloidal damper without attached compression helical spring, for which a Maxwell model, consisted of a dashpot and an elastic element connected in series was considered; and colloidal damper mounted in parallel with a compression helical spring, for which a standard linear model, consisted of a Maxwell unit connected in parallel with an elastic element was considered. Firstly, the vibration transmissibility from the rough road to the vehicle's body for all these suspensions was determined under the constraint that damping varies versus the excitation frequency. Then, the optimal damping and stiffness ratios were decided in order to minimize

the transmissibility of vibration from the rough pavement to the vehicle's body, i.e., to maximize the vehicle's ride comfort.

References

[1] S. K. Jha, "Characteristics and sources of noise and vibration and their control in motor cars", *J. Sound and Vibration*, vol. 47, pp. 543–558, 1976.

[2] N. P. Chironis, *Spring Design and Application*. New York: McGraw-Hill, 1961.

[3] C. M. Harris and C. E. Crede, *Shock and Vibration Handbook*. New York: McGraw-Hill, 1968.

[4] S. Komamura, *Automotive Suspension*. Tokyo: Kayaba Technical, 2005 (in Japanese).

[5] "Mechanical Vibration and Shock – Evaluation of Human Exposure to Whole-Body Vibration". ISO 2631-1, 1997.

[6] D. Bastow, G. Howard and J. P. Whitehead, *Car Suspension and Handling*. New York: SAE International, 2004.

[7] R. F. Kuns, *Automotive Essentials*. New York: Bruce Publisher, 1973.

[8] C. V. Suciu, T. Iwatsubo and S. Deki, "Investigation of a colloidal damper", *J. Colloid and Interface Science*, vol. 259, pp. 62–80, 2003.

[9] C. V. Suciu, T. Iwatsubo and S. Deki, "Novel principle of mechanical energy dissipation; Part 1: Static performances of a colloidal damper", *JSME Int. J.*, vol. C47, pp. 180–188, 2004.

[10] C. V. Suciu and T. Iwatsubo, "Novel principle of mechanical energy dissipation; Part 2: Dynamic performances of a colloidal damper", *JSME Int. J.*, vol. C47, pp. 189–198, 2004.

[11] T. Iwatsubo, C. V. Suciu, M. Ikenaga, and K. Yaguchi, "Dynamic characteristics of a new damping element based on the surface extension principle in nanopores", *J. Sound and Vibration*, vol. 308, pp. 579–590, 2007.

[12] V. A. Eroshenko, "A new paradigm of mechanical energy dissipation; Part 1: Theoretical aspects and practical solutions", Proc. Inst. Mech. Eng., Part D, *J. Automobile Eng.*, vol. 221, pp. 285–300, 2007.

[13] V. A. Eroshenko, I. Piatiletov, L. Coiffard, and V. Stoudenets, "A new paradigm of mechanical energy dissipation; Part 2: Experimental investigation and effectiveness of a novel car damper", Proc. Inst. Mech. Eng., Part D, *J. Automobile Eng.*, vol. 221, pp. 301–312, 2007.

[14] C. V. Suciu and K. Yaguchi, "Endurance tests on a colloidal damper destined to vehicle suspension", *Experimental Mechanics Int. J.*, vol. 49, pp. 383–393, 2009.

[15] C. V. Suciu and T. Tobiishi, "Investigations on the optimum design of a colloidal damper for autovehicle suspension", in *Proc. 9th World Congr. Struct. Multidiscipl. Optim.*, Shizuoka, Japan, CD-ROM, pp. 1–10, 2011.

[16] C. V. Suciu, "Ride-comfort of an automobile equipped with colloidal dampers at its frontal suspension", in *Proc. Int. Conf. on Noise and Vibration Eng.*, Leuven, Belgium, CD-ROM, pp. 4233–4245, 2010.

[17] A. Hac and I. Youn, "Optimal semi-active suspension with preview based on a quarter car model", *Trans ASME, J. Vibration Acoustics*, vol. 114, pp. 84–92, 1992.

[18] A. Hac and I. Youn, "Optimal design of active and semi-active suspensions including time delays and preview", *Trans ASME, J. Vibration Acoustics*, vol. 115, pp. 498–508, 1993.

[19] A. Preumont and K. Seto, *Active Control of Structures*. New York: Wiley, 2008.

Claudiu Valentin Suciu received the Dr.Eng. from Polytechnic University of Bucharest (Romania) in 1997, and Dr.Eng. from Kobe University (Japan) in 2003. Currently, Professor C. V. Suciu works at the Department of of Intelligent Mechanical Engineering. His research interests are in tribological design of various machine elements.
E-mail: suciu@fit.ac.jp
Faculty of Engineering
Department of Intelligent Mechanical Engineering
Fukuoka Institute of Technology
3-30-1 Wajiro-Higashi, Higashi-ku, Fukuoka
811-0295, Japan

Tsubasa Tobiishi is master-course student in Graduate School of Engineering, Fukuoka Institute of Technology.

E-mail: mcm10007@bene.fit.ac.jp
Faculty of Engineering
Department of Intelligent Mechanical Engineering
Fukuoka Institute of Technology
3-30-1 Wajiro-Higashi, Higashi-ku, Fukuoka
811-0295, Japan

Ryouta Morii is master-course student in Graduate School of Engineering, Fukuoka Institute of Technology.

E-mail: mcm11010@bene.fit.ac.jp
Faculty of Engineering
Department of Intelligent Mechanical Engineering
Fukuoka Institute of Technology
3-30-1 Wajiro-Higashi, Higashi-ku, Fukuoka
811-0295, Japan